THE STALL TORQUE OF THE BACTERIAL FLAGELLAR MOTOR

MARKUS MEISTER AND HOWARD C. BERG
Department of Cellular and Developmental Biology, Harvard University, Cambridge, Massachusetts, 02138

ABSTRACT The bacterial flagellar motor couples the flow of protons across the cytoplasmic membrane to the rotation of a helical flagellar filament. Using tethered cells, we have measured the stall torque required to block this rotation and compared it with the torque of the running motor over a wide range of values of proton-motive force and pH. The stall torque and the running torque vary identically: both appear to saturate at large values of the proton-motive force and both decrease at low or high pH. This suggests that up to speeds of ~5 Hz the operation of the motor is not limited by the mobility of its internal components or the rates of proton transfer reactions coupled to flagellar rotation.

INTRODUCTION

A bacterial flagellum is driven by a rotary motor anchored in the cell wall that uses electrochemical energy stored in the transmembrane proton gradient (Berg and Anderson, 1973; Larsen et al., 1974; Berg et al., 1982; Macnab and Aizawa, 1984). Four quantities characterize the process of energy conversion in this engine: the proton-motive force (the free energy per unit charge required to transfer protons into the cell), the proton flux (the number of protons passing through the motor in unit time), the torque (the work per unit angle performed by the flagellar filament), and the speed (the number of revolutions of the filament relative to the cell wall in unit time). Dynamical studies of the flagellar motor have been aimed primarily at exploring the relationship between proton-motive force, torque, and speed. A motile species of *Streptococcus* has proved very useful in these investigations. This bacterium lacks endogenous energy reserves and does not respire. When cells are deprived of a metabolic energy source, the proton-motive force vanishes within 1 h. Then, the cells can be artificially energized, either with a potassium diffusion potential or with a pH-gradient. The rotation of a single flagellum can be studied under light microscopy by tethering a bacterium to a glass surface by one of its flagellar filaments (Silverman and Simon, 1974). This causes the cell body to spin about an axis through the point of attachment at rates up to 10 Hz. The torque generated by the motor can be found by calculating the viscous drag on the rotating cell body.

Here we present a method for measuring the stall torque of the motor, namely the external torque required to stop its rotation. This method relies on the fact that the rotation axis of a tethered cell does not pass through the geometrical center of the cell body. Therefore, one can exert a torque on the body by flowing fluid past the cell. This procedure is illustrated in Fig. 1. Panel *A* is a photomicrograph of a starved cell oriented downstream from its point of attachment by a slow flow of fluid in the direction of the arrow. Panel *B* shows the same cell after glucose was added to the medium: the motor now generates a clockwise torque, yet the flow rate is large enough to block rotation. At lower flow rates, as in panel *C*, the cell body assumes a larger angle of inclination relative to the direction of flow. As the flow rate is decreased further, a critical point is reached where the cell body is oriented at a right angle relative to the direction of the flow (not shown). At all lower flow rates the cell rotates, but, as is evident from the asymmetric image in panel *D*, it moves more slowly during the half-cycle when the motor works against the flow than it does when the motor works with the flow. When the flow is stopped entirely, the cell spins freely. The motor's stall torque can be calculated from the flow velocity at the critical point, the transverse translational drag coefficient of the cell body, and the distance from the tethering axis to the body's center of drag. The motor's running torque can be calculated from the speed of the freely spinning cell and the drag coefficient for rotation of the cell body about the tethering axis.

Manson et al. (1980) measured the speed of tethered cells in media of varying viscosity and found that the torque generated by glycolyzing *Streptococcus* at pH 7.5 is independent of speed within experimental error over the range 0.4 to 8 Hz. The torque developed by artificially energized cells is directly proportional to the applied proton-motive force up to values of ~ -80 mV (Manson et al., 1980; Conley and Berg, 1984; Khan et al., 1985). At a fixed proton-motive force, that torque is independent of temperature, and remains unaltered when the motor is

Dr. Meister's present address is Department of Neurobiology, Stanford University School of Medicine, Stanford, CA 94305.

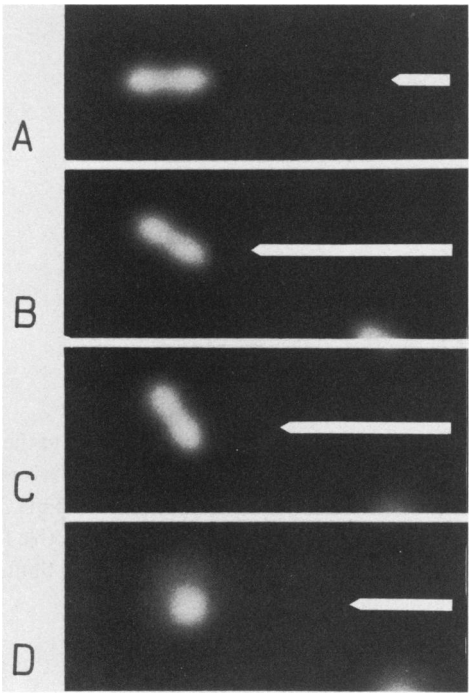

FIGURE 1 Photomicrographs (~7-s exposures) of a tethered cell immersed in a moving fluid. The arrows indicate the direction and relative magnitude of the flow velocity. (*A*) After starvation in buffer A at pH 7.5. (*B*) In the same medium after addition of 0.01 M glucose: the motor generated a clockwise torque, equal and opposite to the torque exerted on the cell body by the flowing medium; the flow velocity near the cell body was ~130 μm/s. (*C*) At a lower flow rate, the cell body stalled at a larger angle relative to the flow. (*D*) At an even lower flow rate, the cell rotated, but it moved more slowly during the upper half of the cycle, as it worked against the flow.

driven by deuterons instead of protons (Khan and Berg, 1983). These observations suggest that rotation of the flagellar filament is tightly coupled to the proton flux through the motor (i.e., that a fixed number of protons carry the motor through each revolution), and that the efficiency of energy conversion at the rotation rates of tethered cells is close to unity (i.e., that the mechanical work performed per revolution is equal to the free energy given up by the protons). Under such conditions one predicts that the work per unit angle, and thus the torque of the motor, is proportional to the proton-motive force, yet independent of temperature and hydrogen isotope, as observed.

Other studies appear to weaken that hypothesis. The swimming speed of *Bacillus subtilis* saturates at large proton-motive force, remaining approximately constant at values above −80 mV (Khan and Macnab, 1980), and drops dramatically at values of the external pH below 6 or above 8.5 (Shioi et al., 1980). Similar effects have been observed with tethered, artificially energized cells of *Streptococcus* (Khan, S., unpublished observations). Why does the torque drop below the value expected from the assumption of tight coupling and high efficiency? A possible explanation is that the motor no longer operates close to thermodynamic equilibrium at extreme values of proton-motive force or pH. Under such conditions its speed might be limited by the rates at which processes that contribute to flagellar rotation can occur, leading to a decrease in the efficiency of energy conversion. For example, the finite mobility of mechanical components of the motor might limit its speed at large proton-motive force. Similarly, if rotation of the filament involves proton transfer to and from moving ligand sites, as has been proposed in several models of the flagellar motor (Läuger, 1977; Oosawa and Masai, 1982; Berg and Khan, 1983), these reactions would proceed more slowly at pH-values far from the dissociation constant of the proton binding sites, which might also cause the efficiency of flagellar rotation to decrease. Under the assumption of tight coupling, none of these limitations would affect the torque generated at stall: the stalled motor is always at thermodynamic equilibrium, since both the flow of protons and the net mechanical movement vanish. Thus, the efficiency of energy conversion approaches unity in the limit of vanishing speed, and one predicts that the stall torque is strictly proportional to the proton-motive force and independent of pH. To test this interpretation of the anomalies in the running torque, we compared the stall torque of tethered cells with their running torque over a wide range of values of proton-motive force and pH.

MATERIALS AND METHODS

Energization of Cells

Cells of *Streptococcus* strain SM29 or SM197, mutants whose motors rotate exclusively clockwise or counterclockwise, respectively (Berg et al., 1982), were grown, washed in buffer A (0.1 M Na_2HPO_4/NaH_2PO_4, 0.2 M KCl, 0.1 mM EDTA) at pH 7.5, sheared, and tethered to a silanized glass coverslip as described by Manson et al. (1980). Their rotational behavior was studied at room temperature. The coverslip was mounted in a flow chamber designed to allow rapid exchange of the external medium (Berg and Block, 1984). The cells were observed by phase-contrast microscopy, and their motion was recorded on video tape. 1 h after harvest all motility had ceased, indicating that no metabolic proton-motive force remained. For experiments on glycolyzing cells we then added glucose to the medium, which initiated rapid rotation of the cell bodies within 1 min. For artificial energization we induced a potassium diffusion potential. Starved cells were exposed to 2 μg/ml valinomycin (a potassium ionophore; Sigma Chemical Co., St. Louis, MO) in buffer A for 2 min. Then a medium of lower potassium concentration, namely a mixture of buffer A and buffer B (0.1 M Na_2HPO_4/NaH_2PO_4, 0.2 M NaCl, 0.1 mM EDTA), was drawn into the flow cell. Under these conditions, the nominal potassium equilibrium potential is determined by the ratio of initial and final potassium concentration as

$$\Delta\psi = \frac{kT}{e} \ln\left(\frac{[K^+]_{final}}{[K^+]_{initial}}\right), \quad (1)$$

where k is Boltzmann's constant, T is the absolute temperature, and e is the electronic charge. In studies of the torque as a function of pH we added 50 mM sodium benzoate (pK_a = 4.19) to the buffers at pH-values below 7.5 and 50 mM methylamine (pK_a = 10.66) at pH-values above 7.5, and allowed the cells to stand for ~30 min before they were shifted to a lower potassium concentration. Benzoate and methylamine permeate the membrane in their uncharged form (cf. Repaske and Adler, 1981; Kihara and Macnab, 1981). This electroneutral exchange of protons

between the cytoplasm and the external medium helps keep the internal pH close to the external value.

Control of Fluid Flow

Fluid was drawn through the chamber with a peristaltic pump (Minipuls 2; Gilson Medical Electronics, Middleton, WI), which was modified so that the roller speed could be controlled by an externally supplied voltage. This signal was provided by a circuit that generated a linear voltage ramp from a high initial value to a low final value. The action of individual rollers compressing the pump tubing led to an additional periodic component in the pump rate, which was suppressed with a surge filter, consisting of ~0.4 cm^3 of air connected to the line between the pump and the flow chamber (cf. Block et al., 1983). After energization, tethered cells were first observed rotating in the absence of fluid flow. After ~20 s the pump was switched to the high flow level, which stalled rotation of most of the cells in the video field. Then the ramp was initiated, and as the flow rate gradually decreased, the tethered cells started spinning one by one. After the final level was reached, the pump was turned off, and we observed the cells rotating for another 20 s. Both the beginning and end of the ramp were marked on the video recording. The entire period of flow lasted ~30 s.

Data Analysis

The video record was analyzed off-line. For the periods before and after the flow, we measured the rotation rate of each spinning cell with a system linked to an Apple II microcomputer that timed the intervals between crossings of the cell's image over a video cursor. The mean of the rotation rates measured before and after the flow was used in the analysis of torque, as described below. For the flow ramp, we determined the time at which each stalled cell first passed through a right angle relative to the direction of flow, just before it initiated its first full revolution. The corresponding volume flow rate through the chamber, which will be called the critical flow rate, was determined from calibrations of the pump rate against the controller voltage.

The Reynolds number characterizing the flow of fluid around a tethered cell is very low, which simplifies the calculations of the torque exerted by the medium on the rotating or stalled cell body. The Navier-Stokes equation is essentially linear in the velocity. Consequently, the torque exerted on a spinning cell is directly proportional to its rotation rate, and the torque exerted on a cell stalled at a right angle to the flow is directly proportional to the critical volume flow rate through the chamber. In most experiments we studied relative changes in the running torque and in the stall torque measured on the same cell when energized under two different sets of conditions. For any particular cell, the ratio of running torques was equal to the ratio of the two rotation rates, and the ratio of stall torques was equal to the ratio of the two critical volume flow rates. We averaged these ratios over all the cells in the sample and computed their mean and standard error. To estimate the absolute running torque, we treated a tethered cell as a circular cylinder rotating in an infinite medium about an axis orthogonal to the cylinder axis. In this approximation the running torque is given by $N_R = (c_R + r^2 c_T)\, 2\pi f$, where c_R is the frictional drag coefficient for rotation about an axis orthogonal to the cylinder axis that passes through its center, c_T is the frictional drag coefficient for translation in a direction orthogonal to the cylinder axis, r is the distance from the rotation axis to the center of the cylinder, and f is the rotation rate (Happel and Brenner, 1965). Similarly, we approximated a cell stalled at the critical point as a stationary cylinder in a fluid whose flow velocity at infinity is homogeneous and orthogonal to the cylinder axis. Thus the torque about the tethering axis is given by $V_S = r\, c_T\, v$, where v is the flow velocity at infinity (Happel and Brenner, 1965). Due to the proximity of the coverslip, the flow velocity actually vanishes on one side of the tethered cell at a distance of the order of a cell width. To take this into account, we chose for v the velocity of the flow at the location of the cell bodies, determined from the initial drift velocity of cells that were torn off the glass by the flow. Although the proximity of the coverslip might introduce significant errors in the estimate of the stall torque, its effect on the calculation of the running torque is probably minor (cf. Jeffery, 1915). The frictional drag coefficients were calculated from the dimensions of the cylinder and the viscosity of the medium according to the formulae of Tirado and de la Torre (1979, 1980). We determined the cell sizes from photomicrographs of the field of tethered cells. Rotating cells generated bright disks on long-term exposures, from whose diameter we deduced the distance between the tethering axis and the center of the cell body.

RESULTS

Absolute Torques

The absolute values of the running torque and the stall torque in a sample of glycolyzing cells are shown in Fig. 2. Running torque and stall torque were clearly correlated, yet showed considerable scatter within the sample of cells, and, on average, the running torque was 3.5 times larger than the stall torque. We suspect that this was due to systematic errors affecting the estimates of torque. In particular, the stall torque is directly proportional to the small distance between the tethering axis and the cell center and thus very sensitive to the measurement of the cell dimensions. The approximations made in calculating the stall torque are affected by the steep velocity gradients near the tethering surface, as described above. Finally, considerable uncertainty is involved in the evaluation of the frictional drag coefficients. For example, when we approximated the cells as ellipsoids instead of cylinders and computed the drag coefficients according to Perrin (1934, 1936), the average ratio of running torque to stall torque dropped to 2.4. Several indications that the stall torque and the running torque are, in fact, equal under these experimental conditions are discussed below.

Relative Torques

None of these systematic errors affect the measurement of relative changes in the running torque or the stall torque

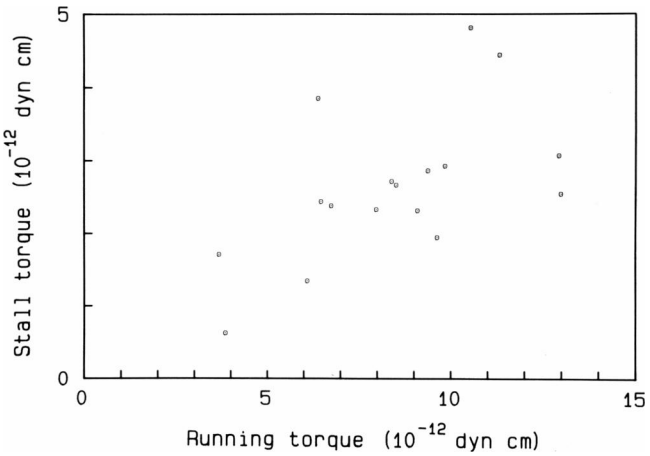

FIGURE 2 The absolute running torque and stall torque of glycolyzing cells of strain SM197. The speed, the critical flow velocity, and the cell dimensions of 17 glycolyzing cells were measured in buffer A that contained 0.01 M glucose at pH 7.5.

generated by the same cell. As long as the geometry of the boundary surface (consisting of the cell surface, the cover slip, and the walls of the chamber) remains unaltered, the running torque is proportional to the rotation rate of the cell body, while the stall torque is proportional to the critical volume flow rate required to stall the cell. Both the rate of rotation and the critical flow rate can be measured with relatively high accuracy, as confirmed by the results obtained on a single glycolyzing cell shown in Fig. 3. During the course of these measurements, the uncoupler 2,4-dinitrophenol (DNP) was added to the buffer at concentrations of 1 or 5 mM. This reduced the proton-motive force, which led to a drop in the rotation rate as well as in the critical flow rate. The stall torque varied proportionally to the running torque, and their correlation was significantly higher than for the data of Fig. 2. Therefore, in subsequent studies, we limited ourselves to the analysis of relative changes in the torques measured on a given cell under various conditions of energization. One of these conditions was chosen as a reference, and all other measurements of rotation rate and critical flow rate were divided by their respective reference values, yielding the changes in the running torque and the stall torque relative to the reference conditions.

We further studied the dependence of the torque on the proton-motive force by energizing starved cells with a potassium diffusion potential, as shown in Fig. 4. The running torque saturated at large nominal values of the proton-motive force, as observed in earlier studies (see Introduction). The stall torque varied in exactly the same manner. Note that this saturation was not due to loss of cytoplasmic potassium, since the torques observed when the cells were returned to 10 mM K^+ were nearly as large as when the cells were first exposed to that concentration. At the end of the experiment, the cells were returned to

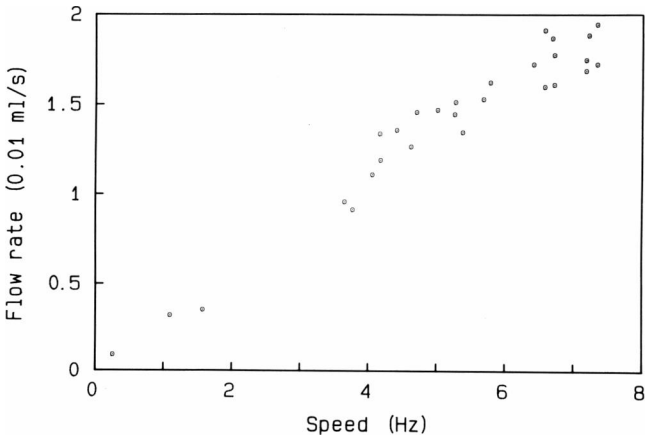

FIGURE 3 The relative running torque and stall torque measured on a single cell of strain SM29. The critical flow rate required to stall the cell was plotted against its speed of rotation in the absence of fluid flow. Initially, the cell was immersed in buffer A that contained 10^{-4} M glucose at pH 7.5. Later, 1 mM DNP and then 5 mM DNP were added to the medium to partially dissipate the proton-motive force.

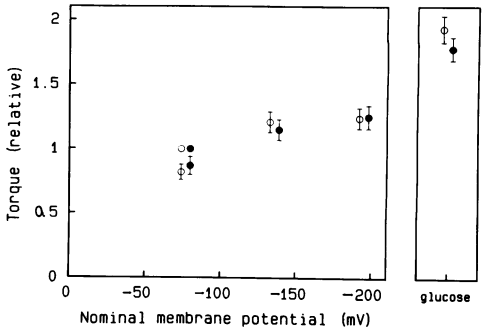

FIGURE 4 The running torque (*open circles*) and the stall torque (*solid circles*) as a function of the potassium diffusion potential. Cells of strain SM197 starved in buffer A that contained 200 mM potassium were treated with valinomycin and shifted sequentially to buffers that contained potassium at the concentrations 10, 1, 0.1, 10, and 200 mM, respectively. Each shift lasted ~80 s, during which we measured speeds and critical flow rates. Then 0.01 M glucose was added to the medium, and speeds and critical flow rates were measured again. For each cell, the speed and the critical flow rate were divided by their respective values observed during the first exposure to 10 mM K^+. The mean and standard error of those ratios were computed over a sample of 25 cells. The nominal membrane potential during artificial energization was calculated from Eq. 1. The symbols for the running torques and stall torques obtained under identical conditions are displaced horizontally for clarity. During the first exposure to 10 mM K^+, corresponding to a relative torque of 1.0, the cells rotated at an average speed of 3.1 Hz.

buffer A that contained 0.01 M glucose, and the torque developed by the glycolyzing cells was found to be ~1.5 times larger than that at a nominal potassium diffusion potential of −195 mV. To compare these torques with those developed by glycolyzing cells that had not been exposed to valinomycin, we tethered another set of cells, supplemented the medium with 0.01 M glucose, and compared the rotation rates before and after treatment with valinomycin. The speeds dropped by a factor of ~1.4, indicating that the torque generated by a glycolyzing cell is $1.5 \times 1.4 = 2.1$ times larger than that at a nominal diffusion potential of −195 mV.

To investigate the behavior of the torque as a function of pH, we energized cells with a potassium diffusion potential first at pH 7.5 and then under conditions where the cytoplasm was buffered by the addition of benzoate or methylamine. The pH of the medium during the second energization was varied, while the first energization served as a reference. As shown in Fig. 5, the running torque dropped significantly at very acidic and very alkaline values of pH. The stall torque showed the same decrease, and its behavior was statistically indistinguishable from that of the running torque. Note that the torque measured at pH 7.5 increased in the presence of methylamine and decreased in the presence of benzoate.

Fig. 6 shows the results of an experiment in which we combined the effects of large proton-motive force and extreme pH. Glycolyzing cells were shifted from pH 7.5 to higher or lower values. The torques were determined immediately after the shift and normalized to the reference

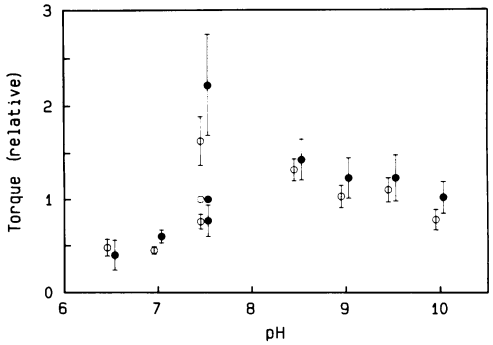

FIGURE 5 The running torque (*open circles*) and the stall torque (*solid circles*) as a function of pH. Starved cells of strain SM197 were first energized at pH 7.5 by a shift from 200 mM K^+ to 10 mM K^+ and back to 200 mM K^+. Then the cells were exposed to a buffer at a different pH that contained 50 mM methylamine (at pH-values above 7.5) or 50 mM sodium benzoate (at pH-values below 7.5). About 30 min later, the cells were energized again by a shift to 10 mM K^+. The relative changes in the running torque and in the stall torque between the first and the second energization were computed, as described in the legend to Fig. 4, and plotted as a function of the pH during the second energization. To control for side effects of methylamine or benzoate, we also performed the second energization at pH 7.5. The upper pair of data points at pH 7.5 was obtained in the presence of methylamine, the lower pair in the presence of benzoate. Each pair of data points corresponds to a different sample of ~10 cells. During the first energization at pH 7.5, corresponding to a relative torque of 1.0, the cells rotated at an average speed of 2.5 Hz.

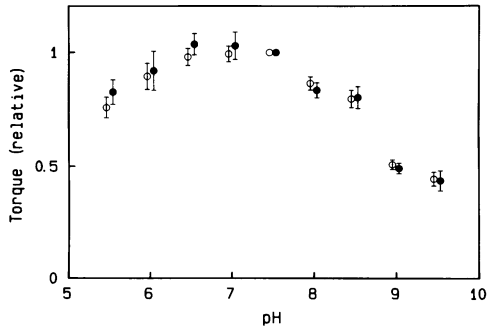

FIGURE 6 The running torque (*open circles*) and the stall torque (*solid circles*) of glycolyzing cells as a function of the external pH. Cells of strain SM 197 in buffer A that contained 0.01 M glucose were observed first at pH 7.5 and then immediately after a shift to a different pH. The corresponding relative changes in the running torque and the stall torque were computed for a sample of 36 cells, as described in the legend to Fig. 4, and plotted as a function of the final pH. During the measurement at pH 7.5, corresponding to a relative torque of 1.0, the cells rotated at an average speed of 5.1 Hz.

values measured at pH 7.5. On the alkaline side, the running torque decreased with increasing pH and extrapolated to zero at ~ pH 10.5, as observed previously (Manson et al., 1980). The running torque increased slightly at pH 6.5, but dropped off as the pH was decreased further. Again, the stall torque varied with pH in exactly the same manner.

DISCUSSION

We have found that the running torque and the stall torque of a tethered cell vary proportionally over a wide range of energization conditions. Although calculations of the absolute running torque and stall torque are affected by large uncertainties, they yield values within the same order of magnitude. However, other studies of the relationship between torque and speed suggest that the stall torque and the running torque are not only proportional but nearly equal. Working with glycolyzing cells of *Streptococcus* at pH 7.5, Manson et al. (1980) found no variation in the torque of a spinning tethered cell over the range of speeds from 8 to 0.4 Hz. It appears unlikely that the motor's behavior should change dramatically between 0.4 and 0 Hz. Recently, Lowe et al. (1987) have investigated the relationship between torque and speed of the motor over a wider range by including measurements performed on swimming cells. The motors of swimming cells rotate much faster than those of tethered cells but generate a smaller torque. For glycolyzing cells at pH 7.5, the torque appears to drop linearly with increasing speed and to vanish at a rotation rate of ~100 Hz (at 24°C). If this linear relationship can be extrapolated back to vanishing speed, the stall torque should be only a few percent larger than the running torque observed at speeds of 5 Hz. Thus it appears likely that the stall torque and the running torque are nearly equal for tethered cells glycolyzing at pH 7.5. We conclude from our measurements that this equality holds also for starved cells energized with very large nominal potassium diffusion potentials or at extreme values of pH.

These results suggest that the saturation of the torque at large nominal proton-motive force and its drop at extreme values of pH are not caused by slow processes coupled directly to flagellar rotation. If the flow of protons and the rotation of the filament are only loosely coupled, the possibility remains that these effects arise from variations in the rates of the leakage processes. For example, Oosawa and Masai (1982) have proposed a model for the flagellar motor that allows for flow of protons and futile cycling of the motor's internal components even when the filament does not rotate. Variations in the rates of these uncoupled processes with proton-motive force or pH could, in principle, affect the stall torque and the running torque in the same manner. If, however, the motor's mechanism couples the flow of protons and the rotation of the filament in a constant ratio, then the stall torque should be strictly proportional to the proton-motive force and independent of the pH, as noted in the Introduction. The data of Figs. 4 and 5 conflict with this prediction. Either the assumption of tight coupling is not justified, or the proton-motive force acting across the cytoplasmic membrane is not equal to the potassium diffusion potential computed from Eq. 1. The fact that the torque of glycolyzing cells is 2.1 times larger than that of artificially energized cells at a nominal membrane potential of −195 mV (see Fig. 4 and Results) lends support to the latter explanation. The proton-motive force of metabolizing bacteria is thought to lie between

−100 and −200 mV, and an average value of −150 mV has been reported in *Streptococcus lactis* (Kashket, 1985). Therefore, it appears very likely that the transmembrane proton-motive force at a nominal potassium diffusion potential of −195 mV is, in fact, much smaller. Other workers have reported difficulties in generating large potassium diffusion potentials. By measuring the distribution of lipophilic cations, Hirota and Imae (1983) determined the proton-motive force of metabolizing cells of an alkalophilic *Bacillus* strain that had been treated with valinomycin and found values significantly below the nominal potassium equilibrium potential for external potassium concentrations below 1 mM. Shioi et al. (1980) reported similar deviations in *Bacillus subtilis*. Kashket and Wilson (1973) suggested that a partial barrier to ion diffusion between the cytoplasmic membrane and the bulk phase of the medium might lead to accumulation of potassium in the restricted space outside the membrane and thus to lower membrane potentials.

The variations of the torque with pH evident in Fig. 5 might similarly reflect difficulties in generating potassium diffusion potentials at extreme pH. Direct damage to the motor, such as the loss of individual torque generating units, is also a possibility, although the decrease in the torque at extreme pH was found to be readily reversible. We do not understand why cells sped up when the medium contained methylamine and slowed down when it contained benzoate (Fig. 5). Since the cells were allowed to stand for 30 min after exposure to either compound, the proton-motive force was close to zero before the change in potassium concentration. The presence of a permeant weak acid or base should have inhibited acidification of the cytoplasm in response to the proton influx and slowed the decay of the proton-motive force after energization. This might explain why the speeds were larger in the presence of methylamine, but it does not account for the deleterious effects of benzoate.

The data in Fig. 6 show that running torque and stall torque vary proportionally even at the large proton-motive force generated by metabolizing cells, but their dependence on the external pH is difficult to interpret. For example, the operation of the ATP-driven proton pump might depend strongly on the external pH. If so, a shift in pH would not only affect the proton concentration gradient but also the membrane potential, which would vary with the rate of proton extrusion by the H^+-ATPase.

In conclusion, we have shown that the stall torque of the flagellar motor is equal to the torque it generates at the speeds of tethered cells over a wide range of experimental conditions. Thus the speed of tethered cells is not limited by the rates of processes contributing to rotation of the flagellar filament. The relationship between the stall torque and the proton-motive force deviates from proportionality under conditions in which it appears likely that the effective proton-motive force available to the motor is smaller than expected from a calculation of the potassium diffusion potential. Such proportionality is predicted by the hypothesis that the flagellar motor tightly couples the flow of protons to rotation of the filament. If the proton-motive force available to the motor could be determined accurately, measurements of the stall torque would allow a stringent test of this hypothesis.

We thank David Blair for his comments on the manuscript.

This work was carried out in the Division of Biology at the California Institute of Technology. This work was supported by a grant from the U.S. National Science Foundation (DMB8518257).

Received for publication 13 February 1987 and in final form 20 May 1987.

REFERENCES

Berg, H. C., and R. A. Anderson. 1973. Bacteria swim by rotating their flagellar filaments. *Nature (Lond.)*. 245:380–382.

Berg, H. C., and S. M. Block. 1984. A miniature flow cell designed for rapid exchange of media under high-power microscope objectives. *J. Gen. Microbiol.* 130:2915–2920.

Berg, H. C., and S. Khan. 1983. A model for the flagellar rotary motor. *In* Mobility and Recognition in Cell Biology. H. Sund and C. Veeger, editors. de Gruyter, Berlin. 485–497.

Berg, H. C., M. D. Manson, and M. P. Conley. 1982. Dynamics and energetics of flagellar rotation in bacteria. *Symp. Soc. Exp. Biol.* 35:1–31.

Block, S. M., J. E. Segall, and H. C. Berg. 1983. Adaptation kinetics in bacterial chemotaxis. *J. Bacteriol.* 154:312–323.

Conley, M. P., and H. C. Berg. 1984. Chemical modification of *Streptococcus* flagellar motors. *J. Bacteriol.* 158:832–843.

Happel, J., and H. Brenner. 1965. Low Reynolds Number Hydrodynamics. Prentice-Hall, Englewood Cliffs, NJ. Chapter 5.

Hirota, N., and Y. Imae. 1983. Na^+-driven flagellar motors of an alkalophilic *Bacillus* strain YN-1. *J. Biol. Chem.* 258:10577–10581.

Jeffery, G. B. 1915. On the steady rotation of a solid of revolution in a viscous fluid. *Proc. Lond. Math. Soc.* 14:327–338.

Kashket, E. R. 1985. The proton motive force in bacteria: a critical assessment of methods. *Annu. Rev. Microbiol.* 39:219–242.

Kashket, E. R., and T. H. Wilson. 1973. Proton-coupled accumulation of galactoside in *Streptococcus lactis* 7962. *Proc. Natl. Acad. Sci. USA.* 70:2866–2869.

Khan, S., and H. C. Berg. 1983. Isotope and thermal effects in chemiosmotic coupling to the flagellar motor of *Streptococcus*. *Cell.* 32:913–919.

Khan, S., and R. M. Macnab. 1980. Proton chemical potential, proton electrical potential, and bacterial motility. *J. Mol. Biol.* 138:599–614.

Khan, S., M. Meister, and H. C. Berg. 1985. Constraints on flagellar rotation. *J. Mol. Biol.* 184:645–656.

Kihara, M., and R. M. Macnab. 1981. Cytoplasmic pH mediates pH taxis and weak-acid repellent taxis of bacteria. *J. Bacteriol.* 145:1209–1221.

Larsen, S. H., J. Adler, J. J. Gargus, and R. W. Hogg. 1974. Chemomechanical coupling without ATP: the source of energy for motility and chemotaxis in bacteria. *Proc. Natl. Acad. Sci. USA.* 71:1239–1243.

Läuger, P. 1977. Ion transport and rotation of bacterial flagella. *Nature (Lond.)*. 268:360–362.

Lowe, G., M. Meister, and H. C. Berg. 1987. Rapid rotation of flagellar bundles in swimming bacteria. *Nature (Lond.)*. 325:637–640.

Macnab, R. M., and S.-I. Aizawa. 1984. Bacterial motility and the bacterial flagellar motor. *Annu. Rev. Biophys. Bioeng.* 13:51–83.

Manson, M. D., P. M. Tedesco, and H. C. Berg. 1980. Energetics of flagellar rotation in bacteria. *J. Mol. Biol.* 138:541–561.

Oosawa, S., and J. Masai. 1982. Mechanism of flagellar motor rotation in bacteria. *J. Physiol. Soc. Jpn.* 51:631–641.

Perrin, F. 1934. Mouvement Brownien d'un ellipsoide. I. Dispersion dielectrique pour des molecules ellipsoidales. *J. de Phys. Radium.* 5:497–511.

Perrin, F. 1936. Mouvement Brownien d'un ellipsoide. II. Rotation libre et depolarisation des fluorescences. Translation et diffusion de molecules ellipsoidales. *J. de Phys. Radium.* 7:1–11.

Repaske, D. R., and J. Adler. 1981. Change in intracellular pH of *Escherichia coli* mediates the chemotactic response to certain attractants and repellents. *J. Bacteriol.* 145:1196–1208.

Shioi, J.-I., S. Matsuura, and Y. Imae. 1980. Quantitative measurements of protonmotive force and motility in *Bacillus subtilis*. *J. Bacteriol.* 144:891–897.

Silverman, M., and M. Simon. 1974. Flagellar rotation and the mechanism of bacterial motility. *Nature (Lond.).* 249:73–74.

Tirado, M. M., and J. G. de la Torre. 1979. Translational friction coefficients of rigid, symmetric top macromolecules. Application to circular cylinders. *J. Chem. Phys.* 71:2581–2587.

Tirado, M. M., and J. G. de la Torre. 1980. Rotational dynamics of rigid, symmetric top macromolecules. Application to circular cylinders. *J. Chem. Phys.* 73:1986–1993.